NANO LETTERS
Letter
Cite This: Nano Lett. 2019, 19, 2598−2602
pubs.acs.org/NanoLett

Force-Dependent Unbinding Rate of Molecular Motors from Stationary Optical Trap Data

Florian Berger,*[,†] Stefan Klumpp,[‡] and Reinhard Lipowsky[§]

[†]Laboratory of Sensory Neuroscience, The Rockefeller University, New York, New York 10065, United States
[‡]Institute for the Dynamics of Complex Systems, Georg-August University Göttingen, 37077 Göttingen, Germany
[§]Theory and Bio-Systems, Max Planck Institute of Colloids and Interfaces, 14424 Potsdam, Germany

Supporting Information

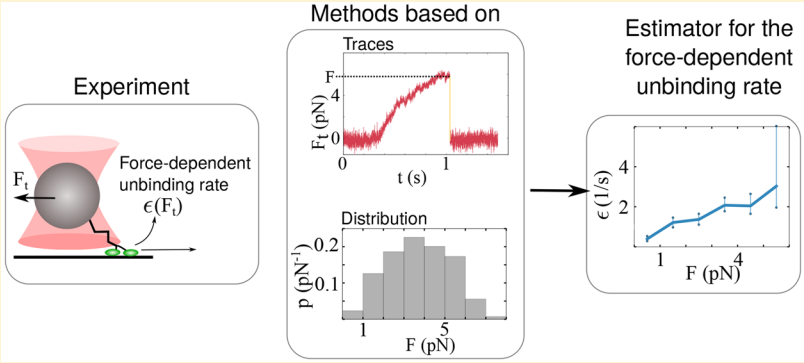

ABSTRACT: Molecular motors walk along filaments until they detach stochastically with a force-dependent unbinding rate. Here, we show how this unbinding rate can be obtained from the analysis of experimental data of molecular motors moving in stationary optical traps. Two complementary methods are presented, based on the analysis of the distribution for the unbinding forces and of the motor's force traces. In the first method, analytically derived force distributions for slip bonds, slip-ideal bonds, and catch bonds are used to fit the cumulative distributions of the unbinding forces. The second method is based on the statistical analysis of the observed force traces. We validate both methods with stochastic simulations and apply them to experimental data for kinesin-1.

KEYWORDS: *Molecular motor, kinesin, optical trap, unbinding rate, dissociation rate, unbinding force*

In mammals, at least 80 genes code for different cytoskeletal motors that transduce chemical free energy into mechanical work.[1,2] These molecular motors perform nanometer steps along filaments from which they unbind stochastically after a finite run length.[3] Both their stepping dynamics and their unbinding behavior are strongly affected by external forces. In cells, these forces arise, for example, from viscous drag, from the elastic coupling to other force-producing molecules, or from their cargo load.[4−6] Thus, stepping and unbinding are characterized by a force−velocity relation and a force-dependent unbinding rate, respectively. These force-dependencies are crucial in order to describe the motor properties in a quantitative manner.

The motor-filament bond of kinesin behaves as a slip bond, that is, the unbinding probability increases with increasing load force. In contrast, the dynein motor may exhibit catch-bond behavior, that is, it may bind to the filament more strongly under force.[7,8] Furthermore, single dynein heads behave as slip-ideal bonds, that is, the unbinding rate first increases with force and then becomes essentially force-independent.[9] Developing reliable methods to determine the force-dependent unbinding behavior of molecular motors is essential to advance our understanding of their functions.

Force spectroscopy probes the dynamics of single molecular bonds. To analyze and interpret data from these experiments, different methods and theories have been developed.[10,11] There are two fundamental differences between typical force-spectroscopic experiments and single-motor experiments; in force spectroscopy, the pulling speed on the molecular bond is set by the experimenter and often kept constant. In contrast, a molecular motor is changing its speed in response to the external force, thus creating a nontrivial feedback between the dynamics and the load force. The second difference between the two experimental setups is the molecular interpretation of the unbinding rate. In force spectroscopy single molecular bonds are probed with well-defined reaction coordinates and the unbinding rate can be considered as a Kramers' escape rate problem.[10−12] In contrast, molecular motors walk along the filament. Depending on the nucleotide state, they change the

Received: January 29, 2019
Revised: March 3, 2019
Published: March 5, 2019

DOI: 10.1021/acs.nanolett.9b00417
Nano Lett. 2019, 19, 2598−2602

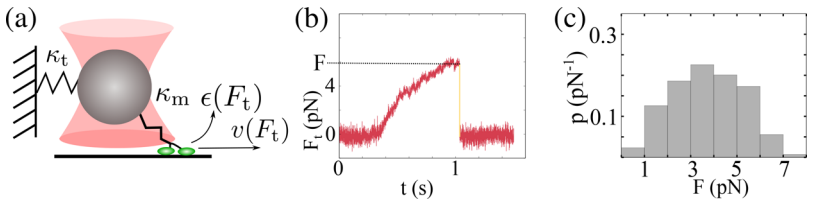

Figure 1. Molecular motor in a stationary optical trap. (a) As the motor pulls the bead out of the trap center with velocity $v(F_t)$, the trapping force F_t on the motor increases and slows the motor down until it stochastically unbinds from the filament at the unbinding force F. The bead falls back to the center of the trap. The stochastic unbinding is governed by the force-dependent unbinding rate $\epsilon(F_t)$. (b) A typical force trace, showing the force as a function of time t, depends on the motor dynamics and on the stiffnesses κ_t and κ_m of trap and motor. The unbinding rate $\epsilon(F_t)$ is an independent motor parameter that reflects the molecular interactions between motor and filament. (c) The histogram of unbinding forces depends on the motor dynamics and on the force-dependent unbinding rate.

bond interaction of their two heads with the filament and the unbinding rate is defined as an effective rate at which both heads unbind from the filament. It is not obvious that methods developed for single bonds can be applied to a coarse-grained description of molecular motors.

Our understanding of how molecular motors respond to external forces is primarily based on single-motor experiments with optical traps.[13] Whereas the force–velocity relations have been studied for a variety of motors,[6,14−17] much less attention has been paid to the force-dependent unbinding rates,[6,7,18] reflecting a lack of reliable and simple methods. Using a sophisticated force-feedback optical trap, the force-dependent unbinding rate has been determined for kinesin-1 as the inverse of the average time the motor is attached to the filament under a constant load force.[7] High-precision experiments that resolve single motor steps allow constructing the force-dependent rates for stepping and for unbinding by directly counting how often these events happen in time.[19,20] However, such experiments are rather challenging and, to resolve single steps, these experiments are often carried out for low, nonphysiological nucleotide concentrations.

The force-dependent unbinding kinetics of a molecular motor is an essential feature of its dynamics and force generation. In fact, the force-dependent unbinding rate together with the force–velocity relation determines the dynamics of a molecular motor in a stationary optical trap. In this Letter, we present a quantitative framework to analyze traces of motors in stationary optical traps and to deduce the force-dependent unbinding rate. In comparison to experiments with force-feedback systems or single-stepping resolution, a stationary optical trap represents a much simpler setup: a single motor pulls a bead against the resisting force generated by a laser trap.[6] While the motor moves away from the center of the trap, the force on the bead increases until the motor unbinds from the filament and the bead snaps back to the trap center, see Figure 1. The force at which the motor unbinds defines the unbinding force and a distribution of these forces can be constructed from many such events. How the shape of the distribution depends on single motor properties and more importantly on the force-dependent unbinding rate is unknown.

In the present Letter, we derive analytical expressions for the probability density of the unbinding forces and relate them to the single motor properties. Comparing these results to experimental data allows us to identify the underlying filament-motor bond behavior. Furthermore, we estimate the force-dependent unbinding rate with a complementary approach based on the statistical analysis of force traces.[6,18] The latter method uses the information on the whole trace and does not require prior knowledge of the motor's elastic properties or of its force–velocity relation. Furthermore, it provides an alternative definition of the force-dependent unbinding rate that is complementary to its commonly used definition as the ratio of velocity to run length.[21] We explicitly show how both methods are connected and discuss their limitations. After validating both methods with stochastic simulations, we apply them to experimental data to determine the force-dependent unbinding behavior of kinesin-1.

Distribution-Based Method. The first method is based on the probability density function $p(F)$ of the unbinding forces as measured experimentally or in simulations. In the following, we will often abbreviate the mathematically precise term "probability density function" by the simpler and more intuitive term "distribution". To derive analytical expressions for this distribution, we extend a method previously used to analyze force–spectroscopic data of single molecules.[11,12] This method transforms the distribution of unbinding forces into the force-dependent unbinding rate

$$\epsilon(F) = \frac{\dot{F}_t(F)p(F)}{1 - \int_0^F p(F')\mathrm{d}F'} \tag{1}$$

in which $\dot{F}_t(F)$ is the force-dependent loading rate, that is, the rate at which the trapping force F_t changes just before it reaches the unbinding force $F_t = F$. From eq 1, we obtain the probability density function

$$p(F) = \frac{\epsilon(F)}{\dot{F}_t(F)}\exp\left[-\int_0^F \frac{\epsilon(F')}{\dot{F}_t(F')}\mathrm{d}F'\right] \tag{2}$$

for the unbinding force. The latter equation implies that the distribution $p(F)$ is determined by the ratio of unbinding rate $\epsilon(F)$ to loading rate $\dot{F}_t(F)$. Therefore, from the distributions for the unbinding force F, we can only estimate the ratio $\epsilon/\dot{F}_t$ as a function of F but not the unbinding rate alone without knowing the loading rate.

However, we can estimate $\dot{F}_t$ from a theoretical description of the motor. In the simplest case, the motor has a linear force–velocity relation $v(F_t) \equiv v_0(1 - F_t/F_s)$ in which F_s is the stall force and v_0 the load-free velocity.[22] The force–extension relation of the motor molecule is assumed to be linear with spring constant κ_m. This spring is connected in series with the spring-like potential of the optical trap described by the spring constant κ_t. Using this motor description, we obtain the force-dependent loading rate $\dot{F}_t(F) = \kappa_{eff}v_0(1 - F/F_s)$ at the unbinding force F with the effective stiffness $\kappa_{eff} \equiv \kappa_m\kappa_t/(\kappa_m + \kappa_t)$. First, we assume that the motor exhibits slip-bond behavior with the unbinding rate $\epsilon(F_t) \equiv \epsilon_0 \exp(F_t/F_d)$, depending on

DOI: 10.1021/acs.nanolett.9b00417
Nano Lett. 2019, 19, 2598−2602

the detachment force F_d and the load-free unbinding rate ϵ_0. For such an unbinding rate, the relation in eq 2 leads to the probability density function

$$p(F) = \frac{F_s \epsilon_0 e^{F/F_d}}{\kappa_{eff} v 0 (F_s - F)} \exp\left[-\frac{F_s \epsilon_0}{\kappa_{eff} v_0} \phi(F)\right] \quad (3)$$

of the unbinding forces with

$$\Phi(F) \equiv e^{F_s/F_d}\left(I\left(\frac{F_s - F}{F_d}\right) - I\left(\frac{F_s}{F_d}\right)\right) \quad (4)$$

and the exponential integral function $I(x) \equiv \int_x^\infty t^{-1} \exp[-t] dt$. In a similar way, we calculate exact expressions for the distributions of unbinding forces corresponding to slip-ideal and catch bonds (Supporting Information). These expressions can be used to fit empirical cumulative distributions constructed from data, thereby estimating the unbinding rate $\epsilon(F)$. To validate our distribution-based approach, we use stochastic simulations to generate data sets of unbinding forces for different types of motor-filament bonds (Supporting Information).

To account for the experimental noise in the traces, we add an appropriate level of noise to the simulated data. In this way, we generate three different data sets for slip, slip-ideal, and catch bonds. We choose the parameter values for the three different bonds such that the resulting unbinding rates have a comparable numerical range, see Figure 2. We then use the analytically derived expressions for the probability density functions $p(F)$ to fit the empirical cumulative distributions of the simulated data and to deduce the parameters of the unbinding rates. The three different force-dependent unbinding behaviors lead to distinct distributions of unbinding forces, see green lines in Figure 2. The estimated parameters are in good agreement with the parameters used to generate the data (Supporting Information). Our fitting procedure accounts for our detection limit of about 0.5 pN for the unbinding forces (Supporting Information). In contrast, the histogram combines all unbinding forces below 1 pN into the first bin and therefore underestimates the distribution, because the data lack forces smaller than the detection limit. Note that the agreement between the predicted distributions and the data is necessarily limited by the assumptions about the underlying microscopic models and by the associated parameterization for the unbinding rates and the motor dynamics. Next, we describe a method that uses the whole ensemble of force traces to estimate the unbinding rate without assuming any microscopic model.

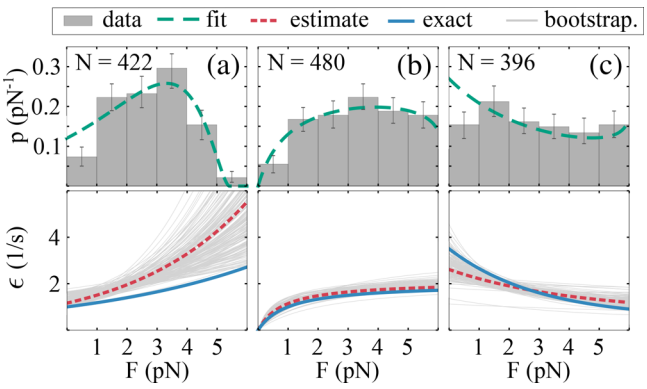

Figure 2. Distribution-based estimate of the unbinding rate (simulation study). From a stochastic simulation of a molecular motor in an optical trap, we obtain a set of unbinding forces from which we construct an empirical cumulative distribution function (Supporting Information). We fit these cumulative distributions by the cumulative distributions as obtained from the analytically derived probability density functions $p(F)$ of the unbinding forces. Optimizing these fits, we obtain the distributions displayed as green lines, which are in good agreement with the gray normalized histograms divided by the bin width for (a) slip bonds, (b) slip-ideal bonds, and (c) catch bonds. The corresponding unbinding rate $\epsilon(F)$ are the red lines in the lower panels. For comparison, we also display the unbinding rates used to generate the data (blue lines). The error bars of the histograms are estimated from a bootstrapping procedure and the gray lines in the lower panels illustrate the variability of the unbinding rate from bootstrapping (Supporting Information).

Trace-Based Method. To estimate the force-dependent unbinding rate from experimental data, without any assumptions about the motor-filament bonds and the force–velocity relation, it is necessary to estimate both the loading rate $\dot{F}_t$ and the distribution $p(F)$ of unbinding forces, see eq 1. The loading rate $\dot{F}_t$ can be estimated from the slope of the force traces before unbinding and $p(F)$ can be estimated by normalizing the histogram of the unbinding forces and dividing this histogram by the bin width.[11] The histogram has N bins with bin width ΔF. The height h_i of the ith bin is determined from the counts C_i per bin as $h_i = C_i/(N^{un}\Delta F)$ with $N^{un} \equiv \sum_i C_i$. An estimator for the force-dependent unbinding rate in eq 1 is then given by[11]

$$\epsilon\left[\left(k - \frac{1}{2}\right)\Delta F\right] = \frac{\dot{F}_t\left[\left(k - \frac{1}{2}\right)\Delta F\right] h_k}{\Delta F\left(\frac{hk}{2} + \sum_{i=k+1}^{N} h_i\right)} \quad (5)$$

This equation involves the force-dependent loading rate $\dot{F}_t\left[\left(k - \frac{1}{2}\right)\Delta F\right]$ which has to be determined from the slopes of the force traces. We rewrite eq 5 in such a way that the unbinding rate can be estimated directly from the data points of the force traces (Supporting Information). We bin the data points of all force traces into N force bins with bin width ΔF and label k. We determine the numbers C_k^{un} of unbinding events and the total number C_k^{to} of data points obtained from all force traces bound to the filament for a given force, which is equal to the total number of data points per force bin. The force-dependent unbinding rate is then given by

$$\epsilon\left[\left(k - \frac{1}{2}\right)\Delta F\right] = \frac{C_k^{un}}{\delta t C_k^{to}} \quad (6)$$

which depends on the time step δt between the recorded points of the trace. Thus, the product $\delta t\, C_k^{to}$ represents the total time of all force traces spent in the kth bin. To evaluate this equation neither a microscopic model nor any kind of fitting procedure is needed, as previously realized in force spectroscopy of a single bond.[23] Applying this approach to our simulated data, we determine the underlying force-dependent unbinding rate solely from the force traces, see Figure 3. Even though the distributions $p(F)$ of the unbinding forces appear to be similar for the slip-ideal and the catch bond, see Figure 2, the trace-based method distinguishes the different unbinding behaviors remarkably well. For small forces, the unbinding rate is underestimated for the slip and the catch bond. This systematic error is a result of the detection limit and the uncertainty about the exact time at which the motor binds to

DOI: 10.1021/acs.nanolett.9b00417
Nano Lett. 2019, 19, 2598−2602

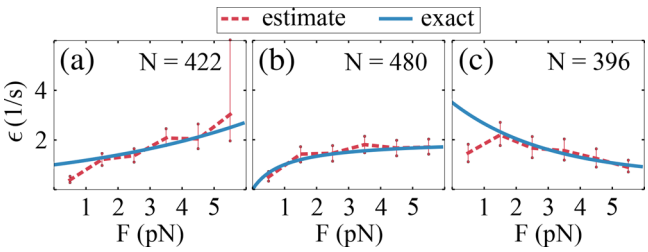

Figure 3. Trace-based estimate of the unbinding rate (simulation study). Without assuming a microscopic model, we only use the unbinding forces and the force traces from the stochastic simulations to estimate the unbinding rate for the three bond behaviors: slip bond (a), slip-ideal bond (b), and catch bond (c). The estimated unbinding rates (red lines) are in very good agreement with the exact unbinding rates used for the simulations (blue lines). The 95% confidence intervals are obtained from bootstrapping (Supporting Information).

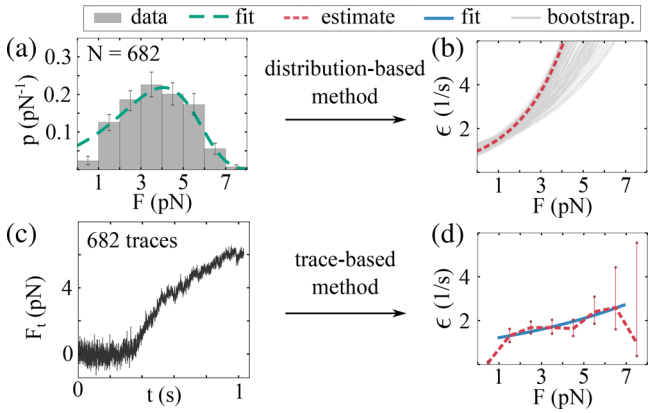

Figure 4. Unbinding rate of kinesin-1 (experimental data). (a,b) *Distribution-based method*: We use the analytical expression in eq 3 for a slip bond to fit the empirical cumulative distribution constructed from the experimental data (Supporting Information). The numerical values of the fitted parameters determine the unbinding-force distribution $p(F)$ (green line in panel a) and the unbinding rate $\epsilon(F)$ (red line in panel b). For comparison, the distribution of the experimental unbinding forces is estimated by a gray histogram. (c,d) *Trace-based method*: We use all 682 force traces, one example trace of the force as a function of time t is shown in (c), to obtain the unbinding rate $\epsilon(F)$ as the red line in (d) from eq 6. Fitting this trace-based estimate with an exponential function (blue line), we obtain the force-free unbinding rate $\epsilon_0 \simeq 1.1\ s^{-1}$ and the detachment force $Fd \simeq 7.4$ pN. In (a) the error bars are obtained from a bootstrapping procedure; in (b), the gray lines illustrate the variability of the unbinding rate from bootstrapping; in (d) the errors are given as 95% confidence intervals (Supporting Information).

the filament (Supporting Information). In case of the slip-ideal bond, the unbinding rate is small for small forces and this systematic error can be ignored.

The Unbinding Rate of Kinesin-1. We apply both methods to experimental data of kinesin-1 pulling a bead out of a stationary optical trap. The data were obtained during control experiments carried out for a previous study.[24] The force-free velocity $v_0 \simeq 484$ nm/s and the trap stiffness $\kappa_t \simeq 0.03$ pN/nm.[24] We assume a motor stiffness of $\kappa_m \simeq 0.3$ pN/nm.[6] However, this assumption is not crucial because the effective stiffness κ_{eff} is dominated by the much smaller trap stiffness κ_t. Using the distribution-based method, we determine the unbinding rate from a fit of the empirical cumulative distribution function constructed from 682 unbinding events, see Figure 4a,b and Supporting Information. Despite our simplifying assumptions about the force-dependent unbinding rate and the motor dynamics, the fit is in good agreement with the data, indicating that kinesin's unbinding rate is consistent with a slip-bond behavior. We find the following optimal parameters with confidence intervals given in brackets: zero-force unbinding rate $\epsilon_0 \simeq 0.97$ [0.80; 1.35] s^{-1}, detachment force $F_d \simeq 2.25$ [2.03; 5.18] pN, and stall force $F_s \simeq 14.97$ [6.26; 15] pN. The latter value for the stall force, as obtained from the distribution-based method, is about twice as large as the experimentally measured value,[14] reflecting our simplified parametrization of the force–velocity relationship (Supporting Information).

Using the trace-based approach, we determine the force-dependent unbinding rate of kinesin-1 from eq 6 as shown in Figure 4d. Because of our detection limit and the associated underestimate of the unbinding rate for the first force bin (Supporting Information), the estimated unbinding rate is inaccurate for forces smaller than 1 pN. Furthermore, the data set includes only six traces with forces exceeding 7 pN and therefore the data are not sufficient to accurately estimate the unbinding rate for forces larger than 7 pN. An exponential fit excluding these boundary points leads to a detachment force of $F_d \simeq 7.4$ pN and a force-free unbinding rate of $\epsilon_0 \simeq 1.1\ s^{-1}$.

Summary and Outlook. We have applied two different computational methods, the distribution-based and the trace-based method, to data from a molecular motor moving in a stationary optical trap. Both methods can be used to estimate the force-dependent unbinding rate from the data. We validated this approach by extensive stochastic simulations. Whereas the distribution-based method gives analytical expressions for the distribution or probability density function $p(F)$ for the unbinding forces, the trace-based method reliably infers the correct unbinding behavior from the simulated data, see Figures 2 and 3.

Furthermore, we have shown that a simple description of kinesin-1 is consistent with the experimental distribution of unbinding forces. Because the trace-based method is more direct and does not rely on model assumptions, our numerical investigations suggest that it provides an accurate estimate of the force-dependent unbinding rate. In contrast, the distribution-based method relies on certain model assumptions. If these assumptions are too simple the estimated parameters are likely to be unreliable (Supporting Information). The trace-based method, which does not involve any assumptions about the functional form of the force dependencies, suggests a force-free unbinding rate of $\epsilon_0 \simeq 1.1\ s^{-1}$ and a detachment force of $F_d \simeq 7.5$ pN. While the unbinding rate is consistent with the value of $\epsilon_0 \simeq 1.0^{-1}$ commonly used for kinesin-1, the detachment force is 2.5 times larger than the value of $F_d \simeq 3$ pN used in most theoretical studies.[22] However, recent experimental and modeling studies indicate a higher value of about 6–7 pN for the detachment force or even a more complicated force dependence.[7,25,26]

Force-dependent unbinding has important consequences for the function of the motors in their cellular environment.[21,27−29] Theoretical descriptions based on single-molecule dynamics indicate that many emerging phenomena, such as cooperative transport and macroscopic force production can only be explained with a suitable force-dependent unbinding rate for the single motors.[30−33]

Our approach provides a systematic framework to study the force-dependent unbinding rate of molecular motors and can

DOI: 10.1021/acs.nanolett.9b00417
Nano Lett. 2019, 19, 2598−2602

be extended to describe more complex optical trapping experiments. To determine the unbinding rate for forces that exceed the stall force, the stage could be moved relative to the trap which adds only one extra term to the loading rate.[9] Such a protocol could improve the statistics for a certain force range and could be used repeatedly to cover a large range of forces.

A first step toward understanding the function of motor proteins is to determine biophysical quantities that are directly accessible to experiments.[34] While the probability distribution of unbinding forces depends on the stiffness of the trap and also on the stiffness of the linker that connects the motor to the bead, the force-dependent unbinding rate is a characteristic property of the motor-filament bond. Therefore, our computational approach provides a systematic framework for future studies to distinguish different motor-filament bonds such as dynein's catch bond from kinesin's slip bond.

■ ASSOCIATED CONTENT

Supporting Information

The Supporting Information is available free of charge on the ACS Publications website at DOI: 10.1021/acs.nanolett.9b00417.

Details of our analytical calculations, descriptions of the simulations, the fitting procedure, and the bootstrapping approach to estimate the data variability, as well as a table of the numerical values for the parameters (PDF)

Python program to generate force traces and to apply the trace-based method to reconstruct the force-dependent unbinding rate (ZIP)

■ AUTHOR INFORMATION

Corresponding Author

*E-mail: fberger@rockefeller.edu.

ORCID

Florian Berger: 0000-0003-3355-4336

Reinhard Lipowsky: 0000-0001-8417-8567

Notes

The authors declare no competing financial interest.

■ ACKNOWLEDGMENTS

We thank Paul Selvin, Hannah A. DeBerg, and Benjamin H. Blehm for providing the experimental data and stimulating discussions. The experimental data were acquired under the support of the NIH. F.B. was supported by a grant from the Alexander von Humboldt-Foundation.

■ REFERENCES

(1) Howard, J. *Mechanics of Motor Proteins and the Cytoskeleton*; Sinauer: Sunderland, MA, 2005.

(2) Schliwa, M.; Woehlke, G. *Nature* **2003**, *422*, 759−765.

(3) Lipowsky, R.; Klumpp, S. *Phys. A* **2005**, *352*, 53−112.

(4) Hunt, A. J.; Gittes, F.; Howard, J. *Biophys. J.* **1994**, *67*, 766−781.

(5) Rogers, A. R.; Driver, J. W.; Constantinou, P. E.; Jamison, D. K.; Diehl, M. R. *Phys. Chem. Chem. Phys.* **2009**, *11*, 4882−4889.

(6) Coppin, C. M.; Pierce, D. W.; Hsu, L.; Vale, R. D. *Proc. Natl. Acad. Sci. U. S. A.* **1997**, *94*, 8539−8544.

(7) Andreasson, J. O.; Milic, B.; Chen, G.; Guydosh, N. R.; Hancock, W. O.; Block, S. M. *eLife* **2015**, *4*, No. e07403.

(8) Rai, A. K.; Rai, A.; Ramaiya, A. J.; Jha, R.; Mallik, R. *Cell* **2013**, *152*, 172−182.

(9) Nicholas, M. P.; Berger, F.; Rao, L.; Brenner, S.; Cho, C.; Gennerich, A. *Proc. Natl. Acad. Sci. U. S. A.* **2015**, *112*, 6371−6376.

(10) Evans, E. *Annu. Rev. Biophys. Biomol. Struct.* **2001**, *30*, 105−128.

(11) Dudko, O. K.; Hummer, G.; Szabo, A. *Proc. Natl. Acad. Sci. U. S. A.* **2008**, *105*, 15755−15760.

(12) Dudko, O. K.; Hummer, G.; Szabo, A. *Phys. Rev. Lett.* **2006**, *96*, 108101.

(13) Veigel, C.; Schmidt, C. F. *Nat. Rev. Mol. Cell Biol.* **2011**, *12*, 163−176.

(14) Carter, N. J.; Cross, R. A. *Nature* **2005**, *435*, 308−312.

(15) Schnitzer, M. J.; Visscher, K.; Block, S. M. *Nat. Cell Biol.* **2000**, *2*, 718−723.

(16) Clemen, A. E.; Vilfan, M.; Jaud, J.; Zhang, J.; Bärmann, M.; Rief, M. *Biophys. J.* **2005**, *88*, 4402−4410.

(17) Gennerich, A.; Carter, A. P.; Reck-Peterson, S. L.; Vale, R. D. *Cell* **2007**, *131*, 952−965.

(18) Thorn, K. S.; Ubersax, J. A.; Vale, R. D. J. *J. Cell Biol.* **2000**, *151*, 1093−1100.

(19) Ali, M. Y.; Vilfan, A.; Trybus, K. M.; Warshaw, D. M. *Biophys. J.* **2016**, *111*, 2228−2240.

(20) Norstrom, M. F.; Smithback, P. A.; Rock, R. S. *J. Biol. Chem.* **2010**, *285*, 26326−26334.

(21) Hancock, W. O. *Nat. Rev. Mol. Cell Biol.* **2014**, *15*, 615−628.

(22) Klumpp, S.; Keller, C.; Berger, F.; Lipowsky, R. In *Multiscale Modeling in Biomechanics and Mechanobiology*; De, S., Hwang, W., Kuhl, E., Eds.; Springer: London, 2015; pp 27−61.

(23) Oberbarnscheidt, L.; Janissen, R.; Oesterhelt, F. *Biophys. J.* **2009**, *97*, L19−L21.

(24) DeBerg, H. A.; Blehm, B. H.; Sheung, J.; Thompson, A. R.; Bookwalter, C. S.; Torabi, S. F.; Schroer, T. A.; Berger, C. L.; Lu, Y.; Trybus, K. M.; Selvin, P. R. *J. Biol. Chem.* **2013**, *288*, 32612−32621.

(25) Arpağ, G.; Shastry, S.; Hancock, W. O.; Tüzel, E. *Biophys. J.* **2014**, *107*, 1896−1904.

(26) Sumi, T. *Sci. Rep.* **2017**, *7*, 1163.

(27) Chaudhary, A. R.; Berger, F.; Berger, C. L.; Hendricks, A. G. *Traffic* **2018**, *19*, 111−121.

(28) Blehm, B. H.; Schroer, T. A.; Trybus, K. M.; Chemla, Y. R.; Selvin, P. R. *Proc. Natl. Acad. Sci. U. S. A.* **2013**, *110*, 3381−3386.

(29) Berger, F.; Keller, C.; Müller, M. J.; Klumpp, S.; Lipowsky, R. *Biochem. Soc. Trans.* **2011**, *39*, 1211−1215.

(30) Berger, F.; Keller, C.; Klumpp, S.; Lipowsky, R. *Phys. Rev. Lett.* **2012**, *108*, 208101.

(31) Klumpp, S.; Lipowsky, R. *Proc. Natl. Acad. Sci. U. S. A.* **2005**, *102*, 17284−17289.

(32) Müller, M. J. I.; Klumpp, S.; Lipowsky, R. *Proc. Natl. Acad. Sci. U. S. A.* **2008**, *105*, 4609−4614.

(33) Berger, F.; Hudspeth, A. J. *PLoS Comput. Biol.* **2017**, *13*, No. e1005566.

(34) Ruhnow, F.; Kloβ, L.; Diez, S. *Biophys. J.* **2017**, *113*, 2433−2443.

DOI: 10.1021/acs.nanolett.9b00417
Nano Lett. 2019, 19, 2598−2602